Using the SAAO Automatic Photometric Telescope to Study the Long-Term Lightcurves of Cataclysmic Variables

Michelle Wiehahn

November 2002

Submitted in partial fulfilment o the requirements for the degree of BSc Honours at the University of Cape Town

Abstract

The SAAO Automatic Photometric Telescope is primarily used for obtaining photometry with a photomultiplier tube. In this project, the feasibility of using the telescope's small acquisition CCD to obtain long-term lightcurves for Cataclysmic Variables is tested. The lightcurves of nine stars are obtained. Six of these are compared to known amateur observations, while the other four, which are members of the Edinburgh-Cape Blue Survey, are classified.

Acknowledgements

Thanks must go to the following people:

Prof. Brian Warner: for the breadth of his knowledge, the depth of his generosity, and the lengths to which he went in extending my hand-in date.

Dr. Patrick Woudt: for knowing everything there is to know about Linux, IRAF, SM and beating computers into submission

Dave Kilkenny: his manual for the APT was not only invaluable, but also priceless. Without his help, there simply wouldn't be a project.

Table of Contents

1 Introduction to Cataclysmic Variables 4
1.1 Evolution of CVs 4
1.2 Outbursts 6

2 The SAAO Automatic Photometric Telescope 9

3 Data Reduction and Analysis 11
3.1 Reduction Process 11
3.2 Analysis and Comparison of Plots 13
3.2.1 AT Ara 13
3.2.2 HP Nor 13
3.2.3 V893 Sco 13
3.2.4 V478 Sco 14
3.2.5 V2400 Oph 14
3.2.6 V436 Cen 14
3.2.7 EC11588 14
3.2.8 EC10565 15
3.2.9 EC10578 15
3.2.10 EC10560 15

4 Conclusion 23

Appendix 24

Bibliography 30

Chapter 1:

Introduction to Cataclysmic Variables

"He also spent some time watching clouds of gas swirl and heat up in the more distant regions of the project"

Terry Pratchett
The Science of Discworld

In this universe of possibilities, a system as quiet and unassuming as our single sun is not as commonplace as we may imagine. To understand why this is, we must look to the formation of stars from the interstellar medium. Our galaxy is filled with vast clouds of gas and dust, which can contract under gravity to form over-dense regions. These regions draw more gas towards themselves, continuing to grow in mass and contract in radius in a cumulative effect. This effect is only halted when core temperatures become hot enough to allow hydrogen to undergo nuclear fission and create helium, releasing large amounts of energy in the process. When the radiative pressure of the released photons in a region of the cloud is sufficient to balance the gravitational pressure in that region, hydrostatic equilibrium is achieved, and a new star is born. However, these stellar nurseries typically contain thousands of solar masses of material. More often than not they collapse to form many over-dense regions, resulting in clusters of new stars, which become gravitationally bound into systems of binary, triplet, and even double binary stars.

Eventually, all stars must evolve. For a solitary star, this is a straightforward affair, and the process is understood well enough. In many binary systems, however, the evolution of one star before the other results in spectacular observational phenomena as the two stars interact, eclipse and distort. There is much that we may learn from the evolution of such systems, and the study of these *cataclysmic variables* (CVs) has been exciting enough to satisfy even the world-weariest of astronomers.

1.1 Evolution of CVs

CVs begin life as a binary system with the separation between the two stars being roughly a few hundred solar radii ($R_\odot$), with an orbital period of about 10 years[1]. The mass of one star is less than one solar mass ($M_\odot$), while the mass of the other is more than 1M. Since the solar lifetime on the main sequence goes as M^{-2}, the heavier star will evolve first. We adopt the convention of labelling this star the *primary*, and the other the *secondary*.

Before moving further, I will briefly introduce the concept of Roche geometry. In a system of two stars, each point in the space around the stars experiences the gravitational forces of the two stars, as well as the centrifugal 'force' of the orbital motion. One may describe the net effect of these forces by means of a three-dimensional system of equipotentials. Projected onto the equatorial plane, these form

a two-dimensional system of contours. Near to the stellar centres, these equipotentials are circular, but on scales comparable to the separation, tidal force considerations alter the shape to almost 'pear-like'. There will be a point in space on the major axis between the two stars where the tips of the two facing 'pears' meet – the *Lagrangian point*, or L_1. This is the saddle point where the three forces mentioned above are exactly balanced. The equipotentials drawn from this point around the two stars are known as their respective *Roche lobes*. Since it is a saddle point, material at L_1 does not need much convincing to flow from one star's potential well to the other's.

This is exactly what happens when the primary expands to become a red giant. Matter transfer to the lighter secondary causes a gain of angular momentum, compensated for by a decrease in the separation between the stars. This results in the primary filling its Roche lobe even more, and the effect is a runaway feedback. The primary literally dumps its entire envelope into the secondary in the space of only a few years. Of course, the secondary hasn't a hope of assimilating the material at this rate, and it too fills its Roche lobe, forming a cloud that encompasses both stars. This is known as the *common envelope* phase, and during this time the binary is effectively orbiting within a red giant. The resulting drag on the stars reduced the orbital energy, causing the separation to decrease from ~100 $R_\odot$ to ~1 $R_\odot$ in about 1000 years[1]. The energy extracted from the binary orbit propels the envelope outward into space, exposing the white-dwarf red-dwarf binary and surrounding it with a *planetary nebula* of illuminated gas.

If the stars are now close enough to each other, the secondary fills its Roche lobe, and the material at L_1 falls into the deeper potential well of the primary. This situation is the opposite of the previous one: the material loses angular momentum, and the separation increases to compensate, breaking the secondary's contact with its Roche lobe. There must be some mechanism of orbital angular momentum loss to sustain mass transfer, and magnetic braking from the secondary's stellar wind and magnetic field provides this. The charged particles of the stellar wind are strung along the magnetic field lines before being released into space, and the long lever arm imparts significant angular momentum to the particles. This angular momentum is obtained from the orbit, and the separation decreases. Another source of angular momentum loss is gravitational radiation, as the energy to generate gravitational waves is also obtained from the orbit.

If mass transfer from the secondary to the primary is sustained, a thin stream of material will issue from L_1 at roughly the speed of sound in the gas (it is the thermal motion of the particles that gives the push they need to escape). The L_1 point is itself orbiting perpendicular to this motion, and the result is that the stream swings into orbit around the primary. The stream sweeps past periastron and eventually meets up with its tail coming the other way. The reunion is a turbulent one, and energy is dissipated by the shocks, leaving the stream to settle into a minimum energy orbit – a circular orbit with the same angular momentum as the material at L_1. As any student of Kepler knows, smaller orbits correspond to higher velocity. The material at the inner edge of the ring is moving faster than the material adjacent to it. The friction causes heating, energy is lost and the material moves into a smaller orbit. Naturally, as the material decreases its orbital radius, it is decreasing its orbital angular momentum, and some material must move outward to balance the books. Thus the

ring of gas spreads out into a disc in the orbital plane of the binary, fed by the secondary and eventually accreting onto the primary.

This is the basic recipe for a cataclysmic variable. There are variations on the theme, but even the simplest of systems is observationally complex. If we are close to the orbital plane, we will see eclipses of not just the primary, but also the disc and the bright spot (the turbulent region where the incoming stream impacts the disc). Observations in the X-ray and ultraviolet regions yield yet more information, but it is the long-term visual lightcurves that are of relevance to this project. To understand these, we must understand the signature characteristic of CVs: the outburst.

1.2 Outbursts

Man has always had a fascination with the *novae stella* – the new stars. The earliest observations of novae come to us from the Orient: China's records (kept for the purposes of portent astrology) date back to the Shang Kingdom in 1500BC[2]; there is evidence that the Tswana tribe in Africa may have been aware of novae or supernovae[3]; and it was Tycho Brahe's observation of the supernova of 1572 that was largely responsible for him resolving to devote his life to astronomy[4]. Yet it is only in the last half century that we have truly been in a position to understand the source of many of these celestial transients.

The periodic brightening of a cataclysmic variable by 3-5 magnitudes is referred to as a 'dwarf nova' outburst, to distinguish it from the more dramatic 'nova eruption', which corresponds to a brightening of 8-15 magnitudes[1]. Observations confirm the wisdom of this classification, as the two types of outburst have different mechanisms and originate in different regions of the CV.

Dwarf novae are amongst the most well documented of CVs, with detailed lightcurves of U Gem going back as far as 1855, and SS Cygni since 1896[5]. The dwarf nova outburst is neatly explained by Osaki's model of disc instability[6]. Observations of eclipsing CVs during outburst show that the disc, rather than the white dwarf and bright spot, dominates the eclipse profile. The dwarf nova is thus a brightening of the disc. Osaki reasoned that if the mass-transfer rate from the secondary were greater than could be effectively transported through the disc, then material would accumulate in the disc. Eventually the excess material would destabilise the disc, increase the viscosity, greatly increase angular momentum transport, and thus spread the material further outwards, as well as further inwards and onto the primary. This will increase the accretion onto the white dwarf surface, enhancing the luminosity of the system and draining the disc of matter, causing the disc to drop back into a quiescent state. The continuing mass transfer will then replenish the disc, until the whole drama re-enacts itself. Osaki's model is well established, with both observational evidence and a sound theoretical model in its favour.

Outburst lightcurves vary in shape even in the same system. Some outbursts are shorter than others, the spacing between outbursts can fluctuate, the speeds of rise and decline change, etc. The reasons for these shape changes involve the radius at which the outburst is triggered, and the distribution of the material left over in the disc after

the previous outburst. Thus careful observation of such outbursts can give us information about the structure of the disc.

With some CVs, the mass transfer rate is so high that the disc is permanently in outburst. These are known as *novalike variables*, or UX UMa stars (used by some to denote the class as a whole, and by others to denote only those novalikes with broad, shallow Balmer lines in the absorption spectra). The high mass-transfer rates seem to be driven by magnetic braking, but a few novalikes are also observed in systems of shorter orbital periods, where gravitational radiation is the key player. The class may also contain pre-novae, post-novae and Z Cam stars for which our observational baseline is too short to reveal other events in their lifetime.

The Z Cam stars are one of two subclasses of dwarf novae that exhibit unusual behaviour. They inhabit the wild frontier between dwarf novae and novalikes. These stars occasionally become caught in outburst for an unpredictable length of time. These periods of novalike steadiness are referred to as standstills. It is thought that they are sensitive to quite small changes in mass-transfer rates. Shortly after outburst, something boosts the mass-transfer rate (possibly heating of the secondary by the luminous disc), forcing the disc into a new equilibrium where it can sustain the heightened mass transfer. After an unpredictable length of time, something else happens to decrease the mass-transfer rate, and the standstill will end with a decline to quiescence. The mass transfer may still be very high for a dwarf nova, and the system may cycle through a quick succession of outbursts, until one triggers yet another standstill.

The SU UMa class of dwarf novae display occasional *superoutbursts* in which the star achieves a brighter state (by ~ 0.7 magnitude) at maximum and remains in outburst for about five times the duration of an ordinary outburst[5]. Photometry of superoutbursts reveals a hump-shaped modulation near superoutburst maximum. Nicholas Vogt first proposed that these *superhumps* were caused by the disc becoming elliptical during superoutbursts[7]. Such an elliptical disc may be expected to precess, with a period longer than the orbital period. There would thus be a beat period between the orbital and precessional periods, and if the superhumps were being caused by an interaction between the disc and the secondary, they would occur at this beat period. Also, parts of the disc would now be orbiting differently from neighbouring regions, and the resulting interactions would dissipate energy, causing the observed brightening during superoutburst. The reason that the disc becomes elliptical in the first place is related to the tidal forces exerted on it by the secondary. These forces are responsible for limiting the outer radius of the disc in the normal situation, but if resonances come into play, the situation may become unstable. If the material in the disc orbits three times for each orbital cycle, the gravitational 'kick' of the secondary will enhance the radial motion of the material, causing the outlying regions of the disc to become elliptical. This particular 3:1 ratio can only exist in CVs where the ratio of the secondary to the primary mass ($M_2/M_1 = q$) is $q \lesssim 0.3$. Since the mass of the secondary star increases as the orbital period increases, SU UMa type stars exist preferentially at low orbital periods.

An interesting characteristic of some novalike lightcurves is a low amplitude brightness modulation over a period of tens of days. All of these modulations are roughly sinusoidal; they do not exhibit rapid rise and decline, or large amplitudes.

They typically vary over a range of 0.7-1.0 mag. This sort of range in a steady state disc requires a factor of ten range in the mass-transfer rate through the disc. These modulations do not appear in dwarf nova, so they probably do not originate with the mass-transfer rate of the secondary. There is a possibility that they are in effect dwarf nova outbursts of low amplitude and large duty cycle[8].

A cataclysmic variable experiences many dwarf-nova outbursts in its lifetime, but less frequent are the dramatic nova eruptions. These are the events that are most likely to be noticed as 'new stars' by the naked eye, with the star brightening by up to 19 magnitudes[5]. The CVs that are observed to undergo such an event are labelled *classical novae.* They typically take 1-3 days to rise to full brightness, but their speed of decline (measured as the time taken to decline by 3 magnitudes) is specific to the star[1]. Some take less than a week to decline, others hundreds of days, and the speed of decline is related to amplitude, with the brightest novae declining fastest.

The cause of the nova eruption originates on the surface of the white dwarf this time. The white dwarf is the surviving core of a star that has long since expended its stores of hydrogen fuel. What remains is mostly helium, with some heavier elements such as carbon, oxygen, neon and magnesium. However, the disc is being supplied by the layer of hydrogen at the surface of the secondary, and this hydrogen is destined to accrete onto the surface of the white dwarf. The surface gravity of the white dwarf is immensely strong, and the material at the base of the accretion layer is crushed under the weight of the gas above. The density at the base of the layer is sufficient to cause degeneracy in the material, forcing the electrons into their lowest energy levels, in accordance with Pauli's exclusion principle. It is this principle – that no more than two electrons of opposite spin may occupy the lowest levels at once – that provides an opposing degeneracy pressure. Eventually, the pressure from the layers above is sufficient to ignite hydrogen burning to helium via the proton-proton chain. In normal matter, this release of energy provides an outward thermal pressure, resulting in an alleviation of the pressure from above. However, in degenerate matter, the pressure is determined by density alone, and the energy only goes to increasing the temperature. When this reaches 2×10^7 K, hydrogen can burn more efficiently through the CNO cycle, the reaction rate of which goes as T^{18}. The thermal runaway thus increases its speed as the temperature climbs to well over 10^8 K. By this point, the energy input is enough to create convection within the layer, sucking down fresh fuel from the higher areas. The temperature will continue to rise until it reaches the Fermi Temperature. At this point the degeneracy is removed, the electrons switch to a Maxwell distribution, and the layer expands catastrophically. The radioactive nuclei deposit their energy into the shell of gas which is now expanding outwards from the primary at a rate of ~1000 kms^{-1}. The hot shell engulfs the binary, and as it cools and expands the outburst slowly fades.

As mentioned before, the speed of decline and the brightness of the nova are specific to the star. This is because the event is dependant upon the mass of the white dwarf. The more massive stars will have a higher surface gravity, and this require less matter to accrete before eruption. Their eruptions will be faster and brighter than those of the less massive white dwarves. Calculations of accretion rates onto the primary combined with the mass of the primary suggest than a CV should experience a nova eruption many times in its life, but the timescale is long compared to our observational records.

Some stars are observed to undergo repeated nova eruptions within the scale of our observations. These *recurrent novae* are mostly thought to be classical novae that have a recurrence time of < 100 years. Some of them may also be more complicated systems of longer orbital periods, where the secondary is an evolved red giant.

In all of the stars mentioned above, the magnetic field of the primary is sufficiently weak that it may be ignored. In another class of CV, know as *polars* (or AM Her stars by some), the magnetic field is so strong that a disc cannot form, leaving the matter to flow from the secondary along the field lines directly onto the surface of the primary. The more interesting – and for that matter more complex – systems are those that lie on the borderline between these cases: the *intermediate polars*, or DQ Her stars.

In the outer regions of some of these intermediate polars, the magnetic field is weak enough to allow a disc to form. In the inner regions, where the field is stronger, the disc separates, streaming along field lines to accrete at either one or both of the magnetic poles of the primary. However, if the magnetic field out at the circularisation radius is strong enough to thread the field lines, no disc will form, and the accretion will be entirely stream-fed. Light from intermediate polars, as with polars, will be polarised by the magnetic field.

Disc formation in an intermediate polar relies on the relative speeds of the magnetic field lines (which are locked to the rotation of the primary) and the speed of the local Keplerian orbit at the point where the material is streamed onto the lines. If the magnetosphere is spinning slower than the material at this point, then the material carries angular momentum onto the primary and spins it up. This will eventually result in the primary attaining a faster rotation period. If the magnetosphere is spinning faster, the material cannot attach to the field lines at this point, as its angular momentum is insufficient. If the field is strong at this point, the rapidly-spinning magnetosphere will expel the material. If the field is weak, an annulus will form, pushing some material inwards to attach to the field lines. In a discless accretor, we have an equilibrium state: the circularisation radius and the corotation radius (the radius at which the magnetic field corotates with the local Keplerian orbit) are the same. This is calculated to occur for $P_{\mathrm{spin}} \sim 0.07 P_{\mathrm{orb}}$. Since there are now two periods involved – both rotational and orbital – we will also encounter beat periods.

Chapter 2:

The SAAO Automatic Photometric Telescope

(or The Little CCD that Could)

"On the other hand, who knows what I'll do?" – Lucy

Charles M. Schulz
You're a Pal, Snoopy

The SAAO APT is also known as the 'Alan Cousins' telescope, which tempts me to nickname this work the 'Alan Cousins Project'. The telescope itself is an Autoscope Corporation 0.75m, and the plans to build it were bought by the SAAO back in the day when they were being sold to universities in a manner that would smack of infomercials today (but wait! Don't call yet! If you buy now, we will include a substantial amount of maintenance to be supplied by you, the valued customer!). A circuit board was also purchased from the company, but everything else was supplied and designed by the SAAO. The system includes a photoelectric photometer; a CCD acquisition system; the Telescope Control System box; the PC running Peter Martinez's 'LINUS' code that controls the telescope and the star field identification; and the PC running a version of Luis Balona's 'LUCY' code that controls the photometry acquisition. They are all housed in a tiny dome at the SAAO Observatory outside Southerland. The scientist responsible for the project at the moment is Dave Kilkenny, and he was kind enough to arrange all of the observations for this project.

When the APT was initially built, it was fitted with a photoelectric system, for high-speed photometry as well as observations for the standard UBVRI system. The telescope was always earmarked to study long-term variables, but with this project we are really testing the abilities and limits of the small acquisition CCD, which was never actually intended to do this kind of work. At the same time, we are exploring the boundaries of the software, as the system is not really set up for CCD reductions. We faced problems right in the beginning with having to get the software to accept that we were just going to be storing a CCD frame. The corrections for this type of input are already to be found in reference (9).

A particularly pleasing feature of the APT's software is Greg Cox's pattern-recognition system, which matches observed star fields to stored star positions, allowing the system to identify fainter target stars. This gives us an advantage over the amateur astronomers (who have played a key role in the study of CVs). Whereas the limit of most amateur telescopes[5] is $m_v \sim 13\text{-}14$, we were hoping to get accurate readings at $m_v \sim 14\text{-}15$. Of course, much of this depended on the quality of the CCD image.

The CCD detector itself is an EEV CCD02-06 system using a 385x576 frame-transfer chip. It is very similar to the systems used on the SAAO 1.9m and 1.0m telescopes, but with a few adaptations. The scale of the CCD is about 2.401 arcsec/pixel in RA and 2.321 arcsec/pixel in DEC.

Chapter 3:

Data Reduction and Analysis

"While the project was indeed only about a foot wide, the space inside seemed to be getting bigger by the second"

Terry Pratchett
The Science of Discworld

3.1 Reduction process

The reduction of CCD images posed an interesting challenge, as no one had ever tried it before on this particular system. Never having used Linux or any CCD reduction system myself, it was a learning process all round. Patrick Woudt suggested that I use IRAF (Image Reduction and Analysis Facility), for its versatility and robustness. The Users' Guide[10] that Patrick secured for me was initially most intimidating. The introduction read: 'if you are a brand-new IRAF user, we recommend that you find some simpler task to work on before proceeding to digital stellar photometry'.

Thanks mostly to Patrick, we eventually worked out a system of reducing the frames, which involved no shortage of twiddling. A full account of the process is documented in the appendix, should anyone want to continue this work. I recommend that until such time as it is better streamlined, this tedious process should only be entrusted to the lowliest of postgraduate students. That said, I will briefly describe the solution, and any suggestions:

The frames arrived 'tarred and gzipped' from Di Cooper's machine, after being forwarded to her by Dave Kilkenny at Sutherland. Theoretically, we should be able to FTP them directly from the APT to Orion, and access them via the Internet from there, but this system is not yet bug-proof.

Filename extensions had to be changed from .fts to .fits, as most of the programs used would not recognise them otherwise.

The frames then had to be flat-fielded. Initially, there was some difficulty in obtaining a suitable flat-field frame, as faint stars were showing up in exposures of both the twilight sky and the Coalsack Nebula. Dave Kilkenny's ingenious solution was to aim the telescope at the black Neoprene lining inside the dome itself. An average of several images yielded a most serviceable flat field, which was used on all of the frames. There was a marked improvement in the quality of the images after flat fielding.

The header files were the next obstacle. IRAF will not recognise certain entries in a header file unless they are in a specific format. The manner in which the APT computers record Right Ascension and Declination, which is as follows:

RA : 17 12 36
DEC : -24 14 44

lead to IRAF reading them as 17:00:00 and –24:00:00 respectively. The colons had to be entered using the **hedit** command in IRAF. Also, the date of observation, which was recorded as dd/mm/yyyy had to be changed to read as yyyy/dd/mm.

Once this was done, the sidereal time had to be calculated by first entering the observatory location as the header word OBSERVAT. Then the airmass and Julian date could be calculated. The process would certainly be faster if these changes were all recorded automatically on site. The RA, DEC and DATEOBS all had to be changed one file at a time, which borders on the ridiculous when you're dealing with hundreds of files.

The CCD frame itself shows the typical saturated areas around the edges and corners. When using the automatic star-finding algorithm **daofind**, the computer returned hundreds of 'stars' in this region. The solution was to either trim the field, or select stars manually. We did both.

Photometry of the stars was done using the **phot** package. We chose an aperture size of 9 pixels, and used the same for all stars and all frames. The minimum and maximum good data values were 10 and 250 respectively.

The photometry was not always successful for every star in the frame. The solution to this was to choose at least four reference stars, with counts/pixel well below the saturation level of 256. Most of the time we were able to get out at least two reference stars which were error-free for 90% of the frames. A handful of frames were useless in this respect, with errors on all stars, and had to be discarded. For HP Nor, we could only secure one reference star for the majority of frames.

Once magnitudes and magnitude errors had been obtained, the plotting program Super Mongo was used to produce plots of magnitude vs. Julian date.

The magnitudes returned by IRAF were in no sense calibrated. In order to do this, we used the AAVSO chart for V2400 Oph, which included several stars of known magnitude in the near region. Two of these (quite blue) stars were within our frames. By doing photometry on these two with IRAF, and then comparing the known to the uncalibrated magnitudes, we were able to obtain the calibration difference of $M=18.15 \pm 0.10$. All magnitudes that appear in figures 1-9 are thus calibrated. The calibrated magnitudes agree with the observed magnitude ranges.

3.2 Analysis and Comparison of Plots

Ten stars were chosen for this project. Six of them are well documented by both amateur and professional astronomers, and were expected to provide a base by which we could judge our results. The other four are of great interest: they are CVs from the Edinburgh-Cape Blue Object Survey, which have only previously been studied by An-Le Chen, for his Ph.D. Thesis at the University of Cape Town. It was expected that the frequently observed systems would give us a good idea for the success of our project, and agreement with the amateur records on the AAVSO site[13] was expected.

The records for some of the stars are shorter than for others, since some of them had already set two months into the project.

3.2.1 AT Ara

We were unfortunate with AT Ara in that a bright, saturated star nearby obscured the image. This did serve to highlight one shortcoming of the APT CCD – its small upper limit of 256 counts/pixel does result in several cases of saturation, and we can therefore not separate out CVs that lie very close to a bright star.

3.2.2 HP Nor (figure 1)

HP Nor is classified as a Z Cam star, and is expected to exhibit outbursts over a period of ~20 days. It has a relatively long orbital period of 17.3 days. Moving from left to right across fig. 1, the first few points appear to be a standstill at first, but comparison with AAVSO data confirms that the star was fainter than 14 in the gap between the first and second data points. Points at HJD+53 and HJD+65 agree with AAVSO points, although this area is somewhat undersampled in their plots, too. Both points appear to be on the decline from outburst. This goes the same for point just before HJD+100. We were unlucky not to catch the star on the rise, or at magnitudes brighter than 13.7, but we did record it to fainter magnitudes than the amateurs, confirming its decline to quiescence at about 16.3 – which is in agreement with the faint end of this star's magnitude range. There is certainly no evidence *against* HP Nor being a Z Cam. We did not directly observe any definite standstills, but the presence of dwarf nova eruptions was confirmed.

3.2.3 V893 Sco (figure 2)

This star is classified as a dwarf nova, or U Gem, with an orbital period of 1.82h. We caught it in decline from outburst at around HJD+10 and HJD+100. Of course, it is far more likely to catch a decline than a rise when observing from night to night, as the rise to outburst is swift and sudden, whereas the decline proceeds over several days. Again, the data is fainter than the AAVSO data, but consistent, as with the smooth drop in magnitude at HJD+30. The behaviour around HJD+55-65 is likely to be caused by short-period flickering in the star itself, as observations from one night

to the next may hit the star at different points in this flickering. Observations thus confirm the classification of V893 Sco as U Gem.

3.2.4 V478 Sco (figure 3)

This star was pushing the limits of our observable magnitude range, as is made evident by the size of the error bars. The lowest official magnitude of this star is 16.7B, so our low points are not inconsistent with this. Yet the size of the error bars makes the exact magnitude of those points difficult to ascertain. V478 Sco is classified as a dwarf nova, but our data does not necessarily agree with this. Particularly, the rise at HJD+150 is far too slow to be that of a dwarf nova eruption. Being so faint, the amateur data was obviously highly undersampled for this star.

3.2.5 V2400 Oph (figure 4)

V2400 Oph is a discless intermediate polar. The period of polarised light is 15.45min, which must be the spin period of the white dwarf, as the magnetic field is locked to the primary, and causes the polarisation. Spectroscopy of the star shows its orbital period to be 3.4h, with a beat period in the X-Ray region at 16.72min. This is caused by the accretion stream flipping between the two magnetic poles as the white dwarf spins beneath it[1]. The spin period of the primary is ~8% of the orbital period, in agreement with calculations for discless accretors. The AAVSO did not have any data for this star over the period in question. However, the star is expected to vary between 14.2V - 14.6V, owing to the spinning of the magnetic field as described above.

3.2.6 V436 Cen (figure 5)

V436 Cen is classified as SU UMa, with an orbital period of 1.56h. With this star, we were very lucky to catch it near the peak of its outburst. AAVSO has it at V=12, in excellent agreement with our data. Regrettably, the star rest of the AAVSO plot over this period was made up entirely of 'fainter thans', giving no useful information for comparison. However, the strong agreement of the outburst is highly encouraging. Of course, with lightcurves of this nature, it would not be possible to observe superhumps unless several observations were made in one night. High-speed photometry (HSP) during outburst would be required to confirm the classification of SU UMa, but this star is definitely a dwarf nova.

3.2.7 EC11588 (figure 6)

Chen classified this star as UX UMa: a novalike variable with broad, shallow absorption Balmer lines in the blue continuum. HSP observations gave a magnitude range of 13 – 13.4, which is in good agreement with our data. There was no evidence of eclipses or any orbital brightness modulation. It was not possible at the time to secure the orbital period. What makes this particular plot interesting is its error bars – at this brightness, we can be sure that what we see is an actual point, and not a spread. The characteristic novalike modulations are thus extremely easy to see.

3.2.8 EC10565 (figure 7)

Chen's spectroscopy revealed broad Balmer emission lines, and HSP observations gave a magnitude range of 15.8 – 16.3, which is in good agreement with our observations. The light curves did show flickering variations with peak-to-peak amplitudes of ~20% on a timescale of a few minutes, which probably explains the variations on the left of the plot. This star remained unclassified by Chen. The absence of HeII λ4686Å and CIII/NIII λ4650Å suggest that it might be a dwarf nova. Two periods were revealed by Fourier analysis: ~12h and ~8h. Chen did not have sufficient data to decide what the orbital period was.

It seems likely from our observations that this star is not a dwarf nova. The rise shown at HJD+40 is too slow to be a dwarf nova eruption. In fact, this star also seems to exhibit the novalike 'waves' as described for EC11588, making it more likely that this star is a novalike.

3.2.9 EC10578 (figure 8)

Chen's spectroscopy revealed weak Balmer lines in emission. He felt that it was probably a novalike, owing to the presence of HeII λ4686Å and CIII/NIII λ4650Å. The HSP observations gave a magnitude range of 15.5 – 15.8. Our data definitely shows a wider range in magnitudes that Chen's, but his runs were quite short. We see the star dipping to about 16.5, and it is likely that this could be an eclipsing system. Owing to Chen's short HSP runs, it is possible that he missed the eclipses. Chen was not able to obtain an orbital period from Fourier analysis. Further HSP observations of this star might yield some interesting data.

3.2.10 EC10560 (figure 9)

Chen's spectroscopy showed strong, broad Balmer emission lines with absorption components in the wings of the higher order, prompting him to classify this star as UX UMa. HSP observations showed a magnitude range of 14 – 14.15. Our observations appear to be a little fainter than this, but they are in good agreement. This star appears to be a very calm, well behaved novalike. Once again, Fourier analysis did not reveal any significant periodicity.

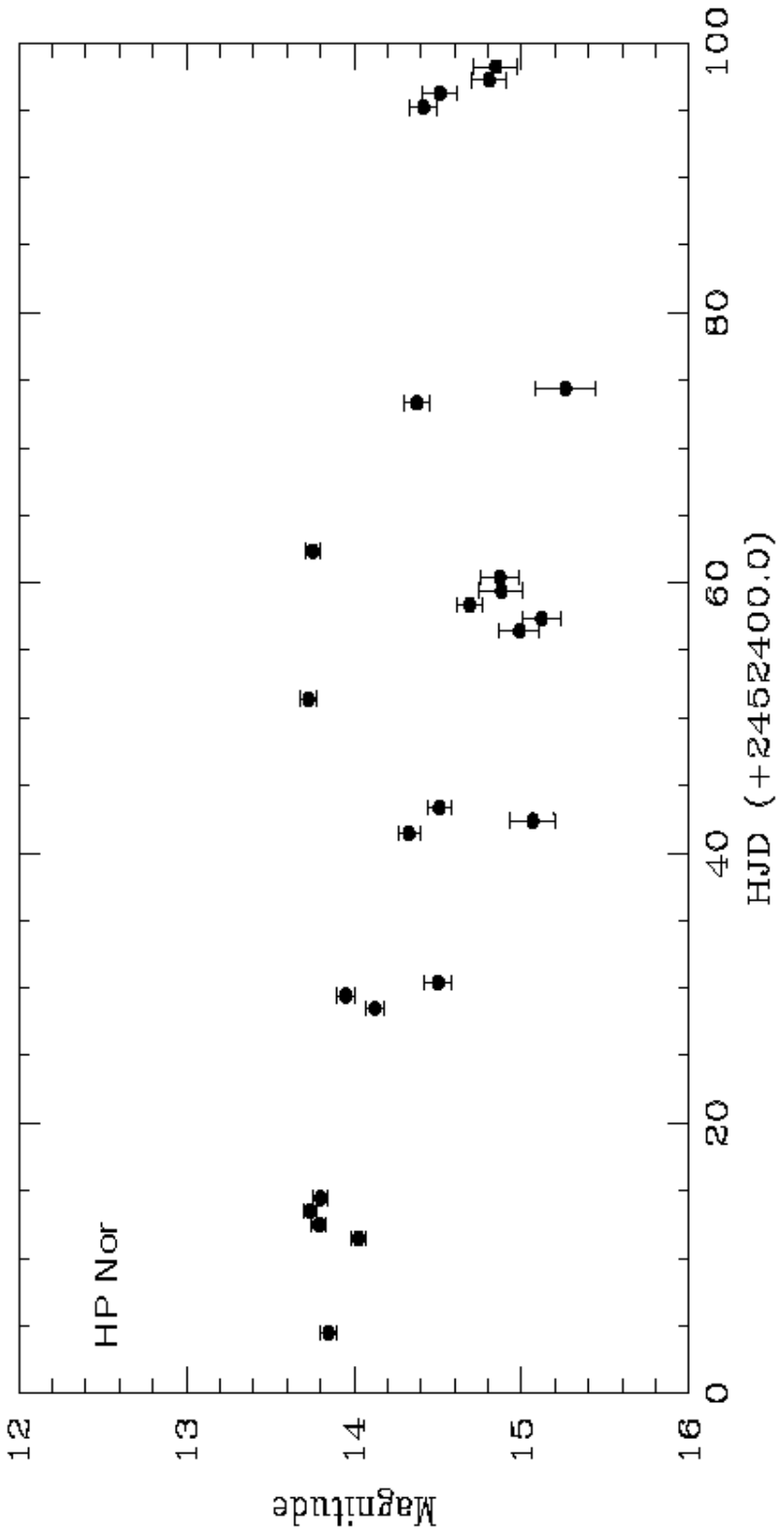

Figure 1: HP Nor

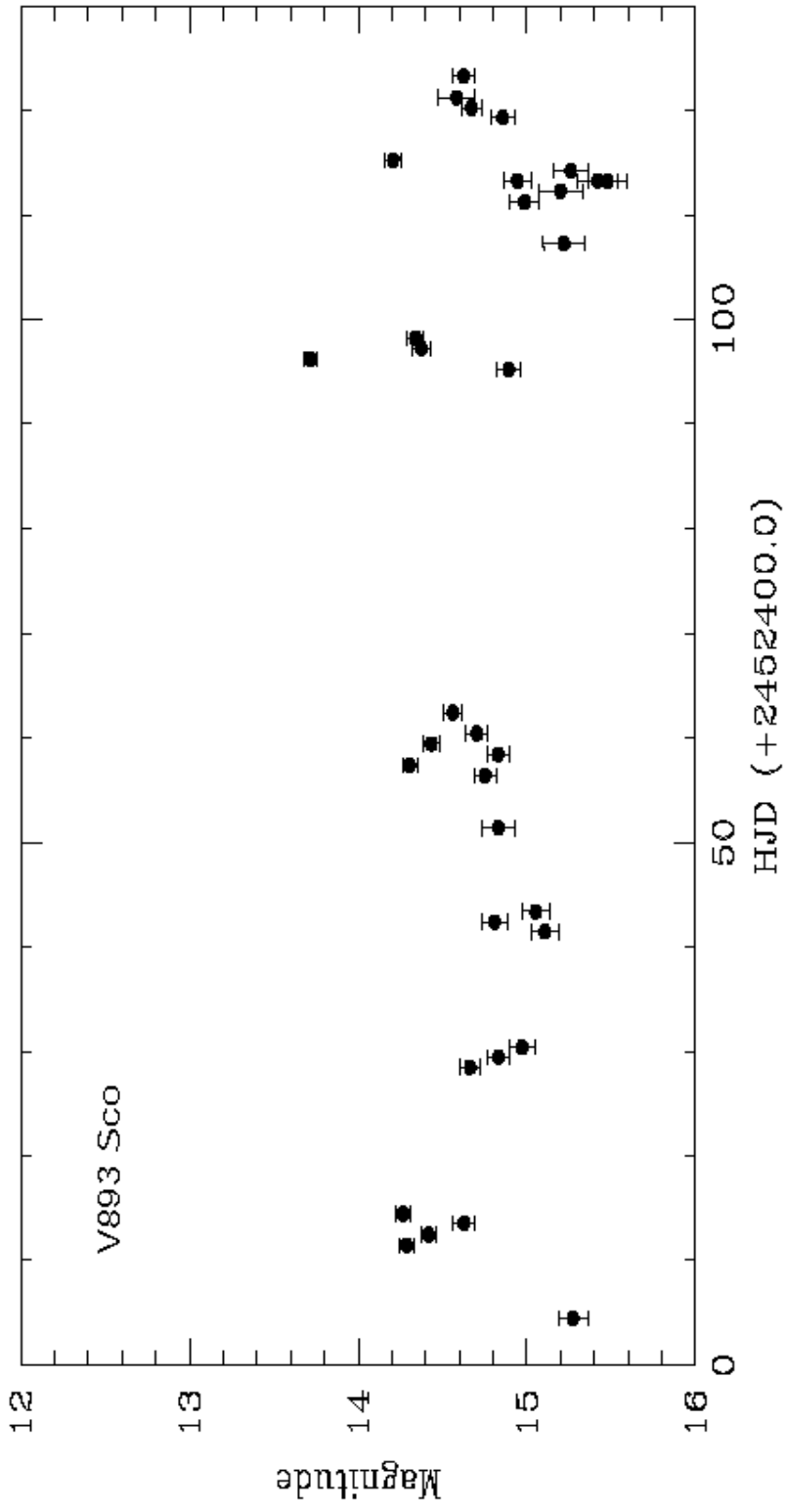

Figure 2: V893 Sco

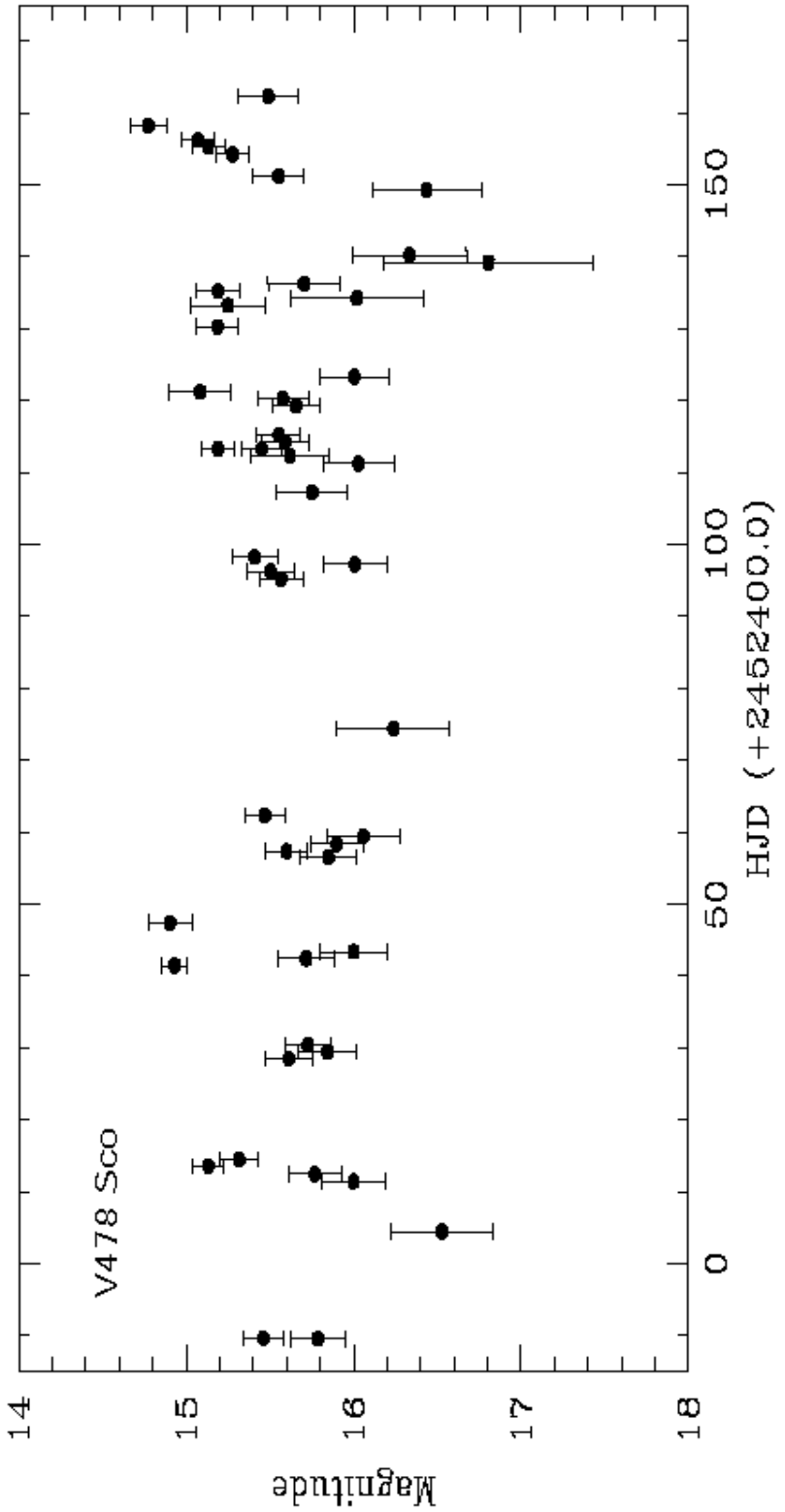

Figure 3: V478 Sco

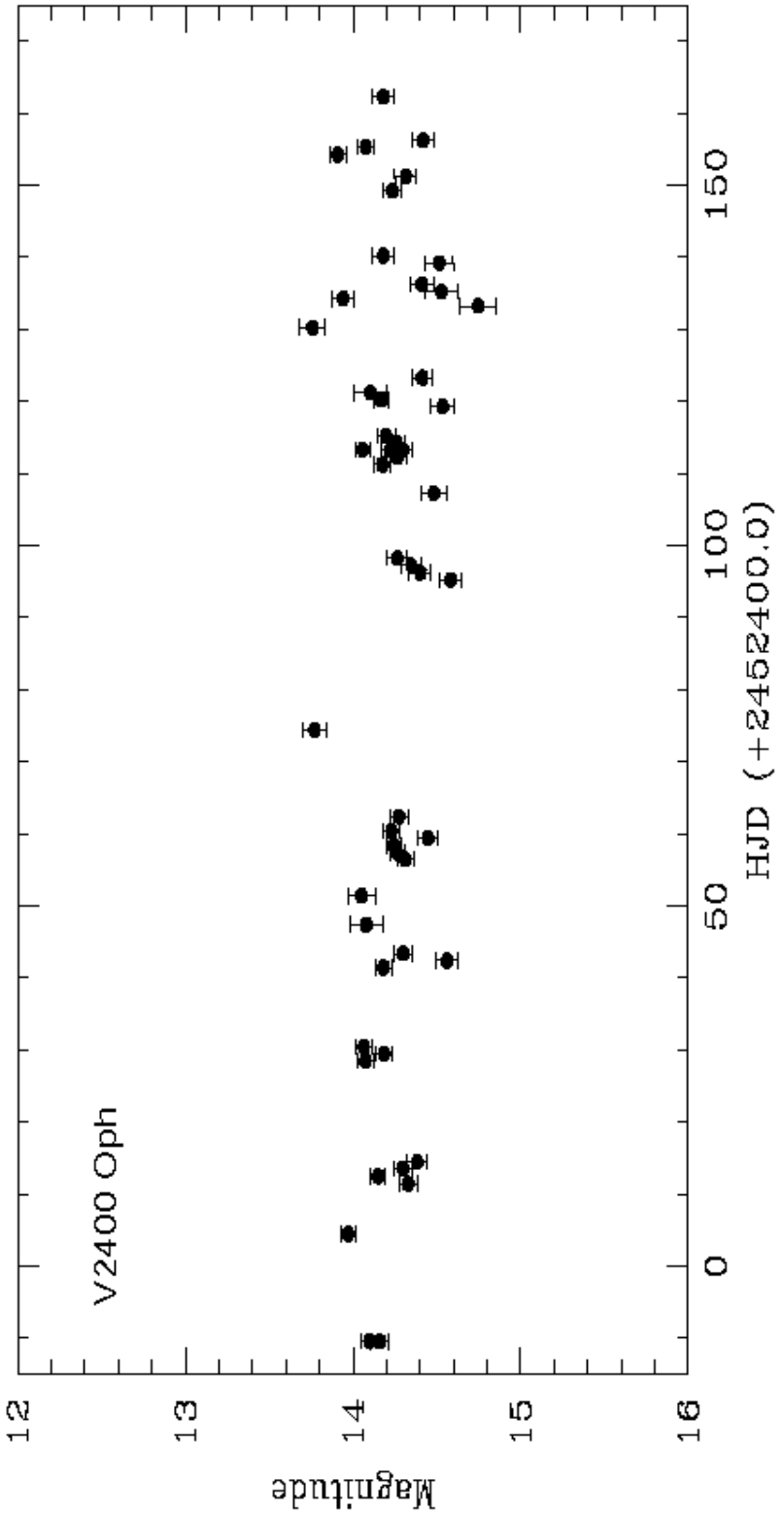

Figure 4: V2400 Oph

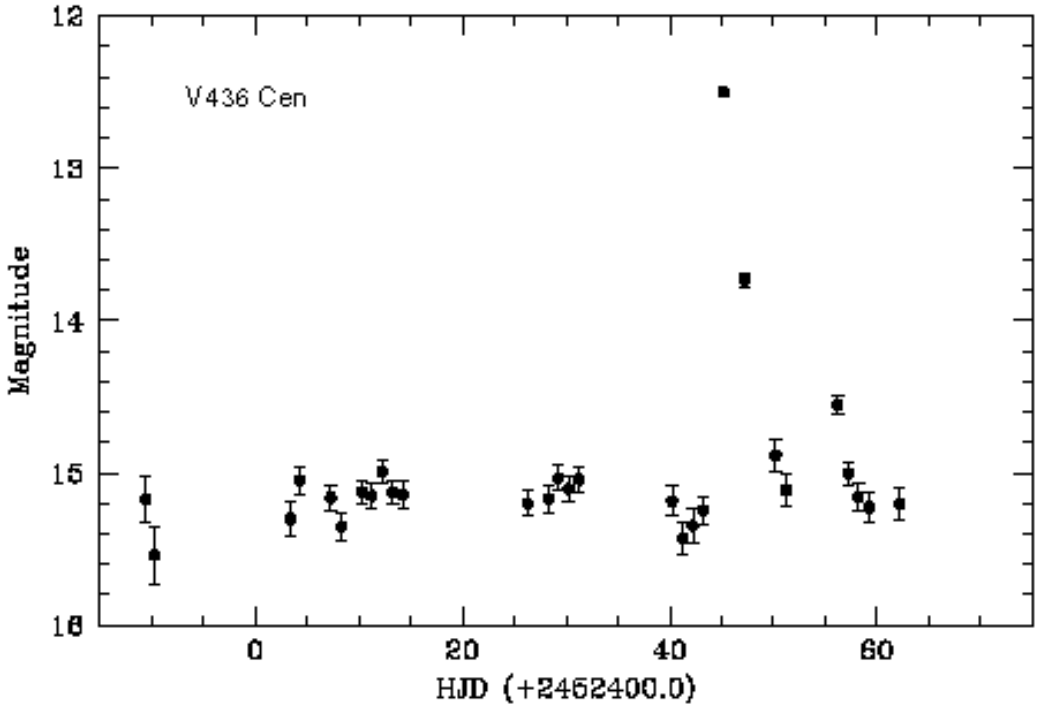

Figure 5: V436 Cen

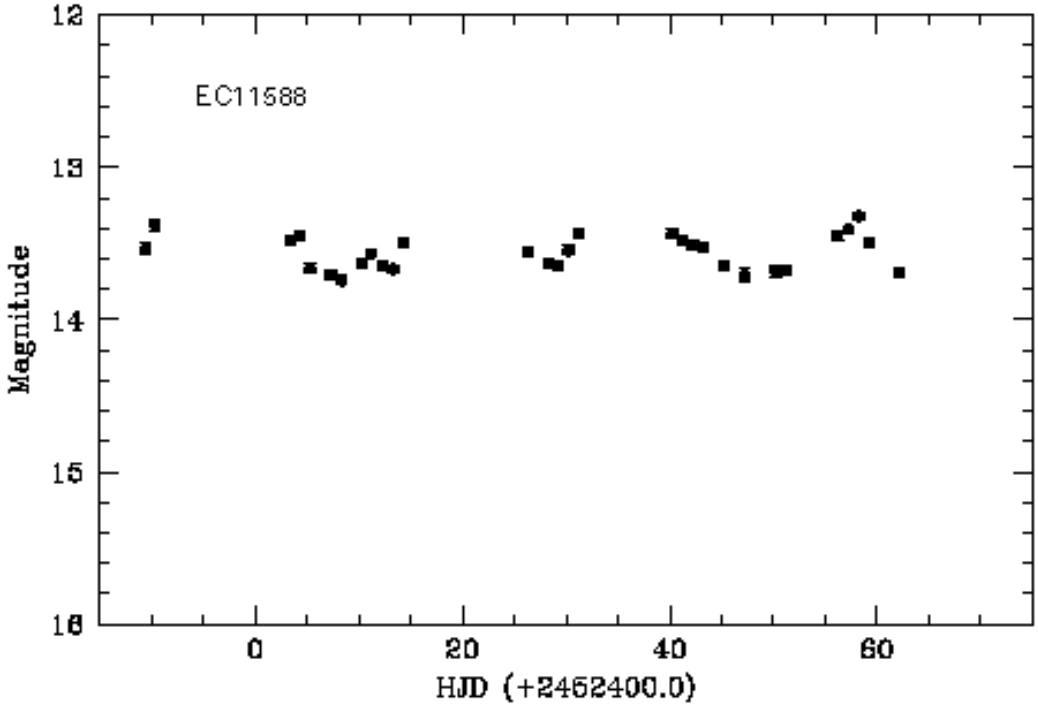

Figure 6: EC11588

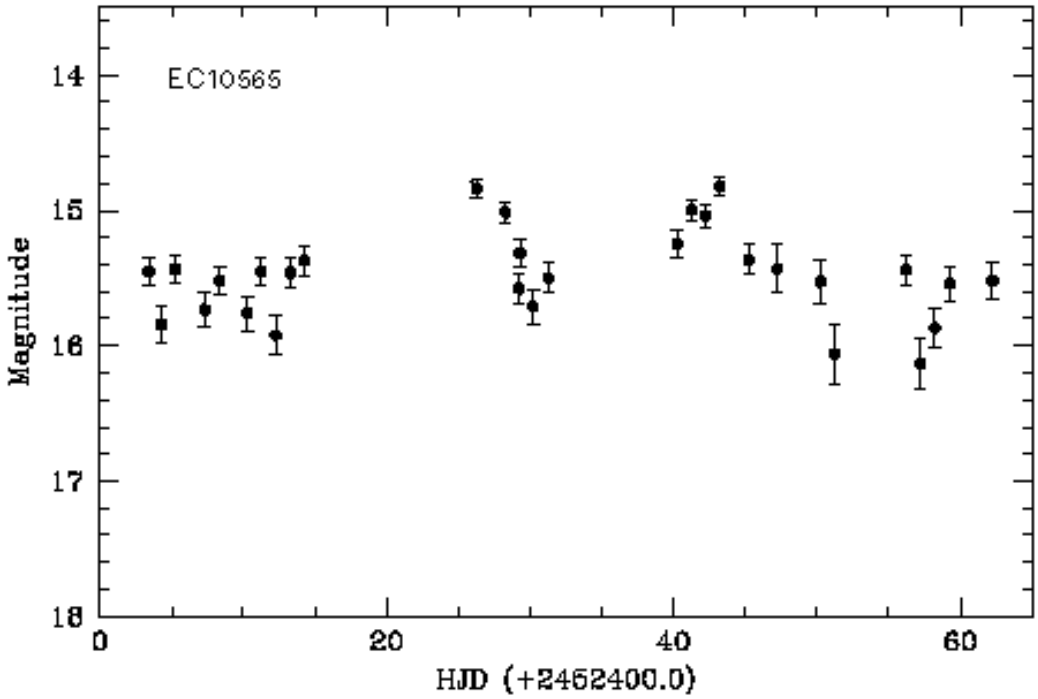

Figure 7: EC10565

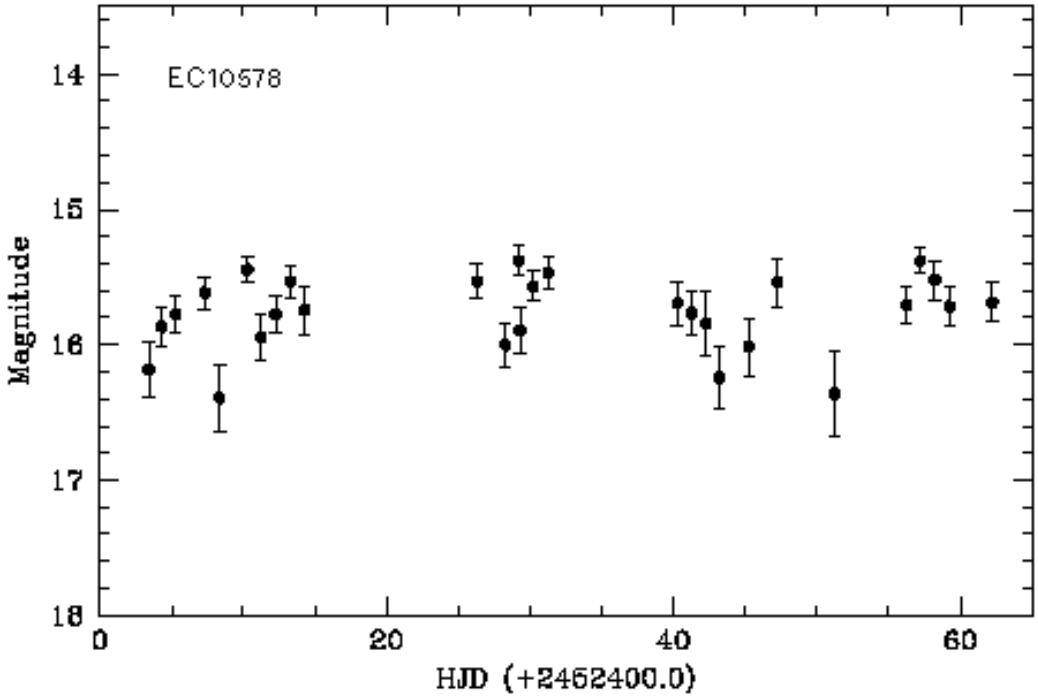

Figure 8: EC10578

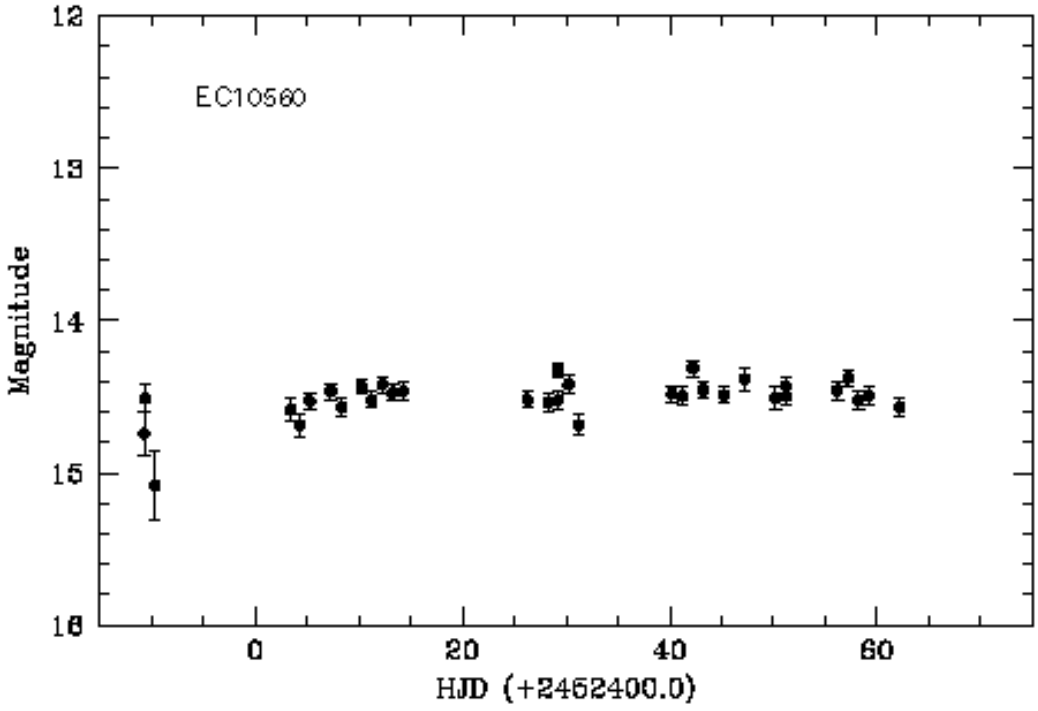

Figure 9: EC10560

Chapter 4:

Conclusion

"The project was nudged gently under a glass dome to prevent any more interference"

Terry Pratchett
The Science of Discworld

In general, this project was a great success. We have shown that we can reliably reach magnitudes as low as 15-16, which is well below the limit of most amateurs. Exposure times of 20-30 seconds were found to be adequate. Our calibration is good, but it could certainly be done more stringently. The APT is kitted out for photometry – it might be an idea to obtain a few photometric observations of some of the stars and use those to calibrate more accurately. The header files, which are written by the computer on site, will certainly require a review if this is to become a regular method of observation, but this is surely a small price to pay for such reliable and simple data. The data were in excellent agreement with the observed AAVSO stars, although regrettable undersampled owing to a shortage of manpower. This should not necessarily be the case, as the operation of the APT can certainly be entrusted to a night assistant or any other astronomers who are willing to lend a hand – obviously after an orientation! Yet I see no reason why we shouldn't be getting data from this telescope just about every night of the year, weather permitting. It can observe many stars in one night, and is the perfect workhorse for long-term lightcurves.

The error bars on our plots were certainly acceptable, ranging from excellent at magnitudes around 13-14, to quite good at about 15.5. One can stretch it to 16, but I wouldn't advise going any fainter than that and expecting anything reliable.

As far as the Edinburgh-Cape objects go, we have had quite exciting results. EC11588 and EC10565 show very good evidence of novalike modulations. EC10578 may well be an eclipsing system, and further study of this star using high-speed photometry would certainly reveal if this were true.

Appendix: Data Reduction Process

"The project promised to offer even greater attractions than staying up all night"
Terry Pratchett
The Science of Discworld

Since this was the first time that anyone attempted to reduce CCD frames from the APT, it was a while before we could work out a method to do so. Thanks mostly to Patrick Woudt, this method exists in the simplest possible form, allowing for our time constraints. Were this to be made into a larger or more permanent project, it might be worth the effort to write a program to automate most of these steps. The changes that had to be made to the header files, as well as the flat-fielding, can be programmed to run automatically at the time of acquisition.

Step 1: ensure that all files have the extension .fits.

Step 2: open IRAF

Step 3: flat-field the images using the command

```
cl> imarith oldfilename/flatfilename newfilename
```

This divides the image by the flat field, and gives it a new name. Provided all the extensions are .fits, you need not write them explicitly when working in IRAF.

Step 4: use the command

```
cl> imhead filename l+
```

to read the header file of an image. If the RA and DEC entries are separated with spaces, you must change the separators to colons, as follows:

```
cl> hedit filename RA '12:01:34' add+ ver-
cl> hedit filename DEC '-37:14:38' add+ ver-
```

If the date of observation is entered at a line called 'date-obs' and has the year at the end, it must be change to 'dateobs' with the year in front, as follow:

```
cl> hedit filename dateobs '2002/04/24' add+ ver-
```

Step 5: To calculate the standard time ST, which is needed to calculated the airmass, one must first set up a file called saao.dat, which reads as follows:

```
observat = "saao"
ut = sexstr ((@'SAST' –2.))
st = mst (@'dateobs', ut, obsdb (observat, "longitude"))
airmass = airmass (ra, dec, st, obsdb (observat, "logitude"))
```

Figure 10: saao.dat

In order to run this file, you must first change to the **astutil** program:

```
cl> noao
no>astutil
```

Once within the **astutil** package, you can edit the **asthedit** function by typing

```
as> epar asthedit
```

Once within the **asthedit** edit facility, ensure that the source file is labelled as 'saao.dat'. Then exit, and execute the following command:

```
as> asthedit filename
```

Step 6: To calculate the julian date

```
as> setjd filename
```

Examples of the header files before and after are shown below.

```
apt38[407,288][short]: EC10560
No bad pixels, min=0., max=0. (old)
Line storage mode, physdim [407,288], length of user area 324 s.u.
Created Fri 12:35:05 28-Jun-2002, Last modified Fri 12:32:40 28-Jun-2002
Pixel file "apt38.fits" [ok]
INSTRUME= APT ACQ CAMERA        /
DATE-OBS= 04/25/2002     /
RA      = 10 58 34        /
DEC     =-29 19 46         /
SAST    = 21:10:17        / South African Standard Time
OBJECT  = EC10560
EPOCH   = 2002.3              / Equinox of RA, Dec
EXPTIME = 020.00                  / Exposure time (sec)
```

Figure 11: Header files as received from APT

```
sflapt38[221,166][real]: EC10560
No bad pixels, min=0., max=0. (old)
Line storage mode, physdim [221,166], length of user area 1215 s.u.
Created Thu 12:11:32 17-Oct-2002, Last modified Thu 12:11:32 17-Oct-2002
Pixel file "sflapt38.fits" [ok]
ORIGIN  = 'NOAO-IRAF FITS Image Kernel July 1999' / FITS file originator
EXTEND  =                    F / File may contain extensions
DATE    = '2002-10-17T10:11:32' / Date FITS file was generated
IRAF-TLM= '12:11:32 (17/10/2002)' / Time of last modification
INSTRUME= APT ACQ CAMERA        /
DATE-OBS= 04/25/2002     /
RA      =            10:58:34
DEC     =           -29:19:47
SAST    = 21:10:17        / South African Standard Time
OBJECT  =             EC10560
EPOCH   = 2002.3                / Equinox of RA, Dec
EXPTIME = 020.00                  / Exposure time (sec)
DATEOBS = '2002-04-25'
OBSERVAT= 'saao    '
UT      = '19:10:17'
ST      = '10:48:02.09'
AIRMASS =     1.00219541244941
JD      =     2452390.29892361
HJD     =      2452390.3028441
LJD     =            2452390.
```

Figure 12: Header file after corrections and calculations described above

Step 7: Change to the daophot package as follows:

```
as> bye
no>digiphot
di>daophot
```

You can now examine the images using the DS9 program, opened in a separate window. To do this, type

```
da> ds9 &
```

Then, once the DS9 window is open, you can display a file using the command

```
da> disp filename
```

At this point, we chopped the image down to exclude the saturated regions. Simply record the coordinates of the new top left and bottom right corners by hovering over the desired points with the mouse (and then writing them down manually – there really wasn't a faster way). Then type the following:

```
da> imcopy oldname[X1:X2,Y1:Y2] newname
```

Step 8: To obtain the coordinates of the reference stars, type **imexam**, then click on the DS9 window. Now hover over a star with the cursor, then press the 'comma' key. A line of information will appear in the first window below the **imexam** command. Do this for all the reference stars, and finally the CV. Then press '**q**'. The stars should have counts below about 200, as brighter stars are likely to be saturated on one or more frames.

Step 9: open a file in which the coordinates of the stars will be stored:

```
da> emacs filename.coo
```

Copy-paste the lines of data that you just recorded using the **imexam** command.

Step 10: type **phot** at the command prompt, and enter the relevant information at the command line. This will calculate magnitudes and errors for all the stars in the .coo file.

Step 11: create a file with the extension .mag, with all the magnitudes and errors of two reference stars and the target star, by copy-pasting. The file should read from left to right:

```
Star1mag  Star1err  Star2mag  Star2err  CVmag  CVerr
```

Step 12: extract the julian date from the header file. This may be done using **imhead** if it is just for one file. If you are using lists, which makes it easier if running through a batch of similar files, then you may want to run a single command into another file and append this file to the .mag file created in step 11. The command to do this is:

```
da> hsel @listname $I,hjd yes > filename.hjd
```

Once finished, the .mag file should read:

```
Star1mag  Star1err  Star2mag  Star2err  CVmag  CVerr  hjd
```

Step 13: We now want the file in a form whereby the julian date is the first column, and is offset by the integer part of the date of first observation. To do this, we create an executable file called 'datechange', with the following contents (this is one line of code, run-on):

```
awk –F" " ' {if ($8>0.) {printf ("%12.8f %6.3f %5.3f %6.3f %5.3f %6.3f %5.3f \n, (($8 – 2452389.0), $2,$3,$4,$5,$6,$7)}}' filename.mag > filename.dat
```

Figure 13: datechange executable file

Step 14: Write the following file, with the extension .sm, in order to plot the data using Super Mongo:

```
location 5000 31000 5000 22000

limits –15 175 16 12

data V2400Oph.dat
read jd 1
read star1 2
read star2 4
read v24 6
read v24err 7
set jd2=jd-11

stats star1 me si ku
echo $me, $si
stats star2 me si ku
echo $me, $si

set off=((star1+4.731) + (star2+4.275))/2.0
set v24cal=v24-off+18.15

ctype black
ptype 12 3
expand 1.1
box
xlabel HJD (+2452400.0)
ylabel Magnitude
expand 1.1

points jd2 v24cal
errorbar jd2 v24cal v24err 2
errorbar jd2 v24cal v24err 4
expand 1
relocate 10 12.5
putlabel 5 V2400 Oph
```

Figure 14: SM file used to plot graph in fig.4

The limits in line 3 of figure 14 are obviously to be chosen based on the limits of magnitude and the time period in question. The variable jd2 in line 11 is the julian date in the .dat file, offset against a chosen base date of jd = 2452400.0. In the example above, this corresponds to a difference of 11 days (in other words, the first day of observation was 2452389.0).

Lines 13-16 calculate mean and standard deviation of the reference star magnitudes, and print them to screen. These mean magnitudes are required for line 18, so it is best to run the first 16 lines of this file first, to obtain these values.

In line 19, we calibrate the magnitude of the CV, first by the offset calculated for the reference stars, and then by the calibration magnitude of 18.15.

Bibliography

1) Hellier, C. 2001. *Cataclysmic Variable Stars: How and Why they Vary*. Springer-Praxis
2) Clark, D.H. and Stephenson, F.R. 1977. *The Historical Supernovae*. Pergamon Press
3) Breutz, P.L. 1969. Sotho-Tswana celestial concepts. *Ethnological Publications*, no. 52, 199. Pretoria: Department of Bantu Administration and Development, Government Printer.
4) Swerdlow, N.M. 1996. 'Astronomy in the Renaissance'. *Astronomy Before the Telescope*. British Museum Press.
5) Warner, B. 1995. *Cataclysmic Variable Stars*. Cambridge University Press
6) Osaki, Y. 1974. PASJ, 26, 429
7) Vogt, N. 1982. ApJ, 252, 653
8) Warner, B. 1994, Astrophysics and Space Sciences, 230, 83
9) Kilkenny, D., Martinez, P. and Carter, D. 2002. *The SAAO Automatic Photometric Telescope*, Version 1. (Unpublished, used with the authors' permission)
10) Davis, L.E. and Massey, P. 1992. *A User's Guide to Stellar CCD Photometry with IRAF*
11) Chen, A. 1994. *A Survey of Cataclysmic Variables from the Edinburgh-Cape Survey*. Ph.D. Thesis, University of Cape Town
12) McBride, V. 2001. *Investigation of Dwarf Nova and Quasiperiodic Oscillations in V436 Cen*. Honours project, University of Cape Town
13) American Association of Variable Star Observer (AAVSO): www.aavso.org